

ORIGINAL ARTICLE

Nobuo Sobue · Minori Fujita · Atsuko Nakano
Tomohiro Suzuki

Identification of defect position in a wooden beam from the power spectrum of longitudinal vibration

Received: April 15, 2009 / Accepted: August 24, 2009 / Published online: December 11, 2009

Abstract The inverse solution procedure that enables the identification of the defect position in a beam from the resonance frequency was exploited. Resonance frequency shifts of a power spectrum due to defects in a longitudinally vibrating beam when both ends are free were investigated by both numerical and experimental analysis. Calculation by a transfer matrix method showed that the frequency shift was large when the defect position coincides with a node of vibration and that no shift occurs when it coincides with a loop of vibration. The frequency shift could be approximated by a sinusoidal curve. Calculation results agreed well with those of the experiment in which artificial round holes were drilled as the defect model. Experimental equations predicting the amount of the frequency shift in function of the defect position were obtained. In the inverse procedure, the defect position was determined by comparing the resonance frequencies between the experimental and estimated power spectra so that the coincidence factor $S(x)$ became a minimum. The results showed the validity of the proposed method to identify the defect positions of fewer than two predominant defects.

Key words Longitudinal vibration · Power spectrum · Identification of defect · Transfer matrix method · Inverse problem

Introduction

Existence of a defect that affects the strength of a structural timber such as a knot induces a resonance frequency shift of vibration.^{1–3} Numerical calculation using a finite-element

method has been applied to the problem.³ Several ideas that aim for the identification of a local defect have been proposed, for example, the flexural curve of a beam in static bending test⁴ and the flexural curve associated with a transfer function in flexural vibration.^{5–7} In the Japanese wood industry, the major type of stress grading machine for sawn timbers for Japanese wooden construction has recently shifted into the longitudinal vibration type machines using a tapping excitation, because the dimension of the structural timber in traditional Japanese construction is larger than that of the 2 by 4 foot timbers used in wood construction in North America.

The merit using the power spectrum of the vibration is that the spectrum can be obtained from a transient sound caused by one hit of a hammer. This method is easily introduced into a current stress grading machine of the longitudinal vibration type because the frequency data have been supplied from a fast Fourier transform (FFT) analyzer included in the dynamic stress grading machine. In this article, the effects of defects on the frequency shift of the power spectrum were estimated by means of a transfer matrix method. Moreover, experimental work was conducted by introducing artificial round holes as structural defects. Then, the prediction of defect position was examined. The defect position was inversely identified from the coincidence test of the power spectrum between the experimental data and calculation by the transfer matrix method.

Theory

Transfer matrix method

The transfer matrix method is a practical tool for solving vibration problems of nonuniform cross-sectional bodies.⁸ This tool has been used in the vibration analyses of wood members such as slender logs,⁹ plywood-webbed box beams,¹⁰ the sound boards of a marimba,¹¹ and the flattening of a resonance frequency shift by defect.⁹ In the transfer

N. Sobue (✉) · M. Fujita · A. Nakano · T. Suzuki
Faculty of Agriculture, Shizuoka University, 836 Ohya, Suruga-ku,
Shizuoka 422-8529, Japan
Tel. +81-54-238-4855; Fax +81-54-237-3028
e-mail: afnsobu@agr.shizuoka.ac.jp

A part of this paper was presented at the 51st annual meeting of the Japan Wood Research Society, 2001, Tokyo

matrix method,⁸ a body is considered to be a linear combination of spring elements and point mass elements. Under the boundary condition of both ends free, the solution with respect to frequency is the resonance frequency to be obtained. In the calculation, the effect of the defect is evaluated as a decrease of a Young's modulus of the corresponding local field matrix. Here, Hatter's FORTRAN program of the torsional vibration problem⁸ was rewritten into a BASIC program and modified to adopt it for longitudinal vibration of a beam subjected to the both ends free condition. A similar numerical calculation using a finite-element method has been applied to the same problem of frequency shift by defects.³

Identification of defect position

General strategy

When the defect position is known, the resonance frequencies are given from the calculation results, as shown later. However, identification of the defect position from the power spectrum is a complicated problem. Our strategy is based on the following method of least squares. The defect position x is determined so that the differences of the resonance frequencies between the experimental and estimated spectra become minimum. The following coincidence factor, $S(x)$, is defined as a parameter of identification.

A relative frequency shift of an arbitrary vibration mode, rsf_n , due to a defect is given by

$$rsf_n = \frac{fr_n - fr_{n,0}}{fr_{n,0}} \times 100 = \frac{fr_n - nfr_{1,0}}{nfr_{1,0}} \times 100 \quad (\%) \quad (1)$$

where fr_n is an experimental resonance frequency of an n th mode of a specimen with a defect, and then $fr_{n,0}$ and $fr_{1,0}$ are resonance frequencies of an n th and the fundamental modes in a defect-free condition, respectively. In our calculation model, the following relative frequency shift $k_n(x)$ is given as a function of the defect position x ($0 \leq x \leq 1$):

$$k_n(x) = \frac{fr'_n(x) - nfr'_{1,0}}{nfr'_{1,0}} \times 100 \quad (2)$$

where $fr'_n(x)$ and $fr'_{1,0}$ are the resonance frequencies of the n th mode given from the result of the transfer matrix method later. The value x that gives the minimum value of $S(x)$ in Eq. 3, the coincidence factor, is the optimal solution of the defect position.

$$S(x) = \{rsf_1 - k_1(x)\}^2 + \{rsf_2 - k_2(x)\}^2 + \dots + \{rsf_N - k_N(x)\}^2 = \sum_{n=1}^N \{rsf_n - k_n(x)\}^2 \quad (3)$$

where N is the highest vibration mode to be considered. In this article, $N = 5$. A piece of information given by one resonance frequency may be too poor to identify the defect position, but integration of information of several vibration modes would increase the degree of confidence on the identification of the defect positions.

Coincidence factor in a two-holes case

Assuming an additional low in the frequency shift, the whole frequency shift of the n th vibration mode $Rsfn$ when the number of holes is two is given by the summation of the effect of each hole.

$$Rsfn = rsfn^{(1)} + rsfn^{(2)} \quad (4)$$

where the superscripts (1) and (2) are the number of the two holes.

The verification of this assumption is proved in this experiment later.

The coincidence factor in the two-holes system is extended from Eq. 3 as follows:

$$S(x_1, x_2) = \sum_{n=1}^N [Rsfn - \{k_n(x_1) + k_n(x_2)\}]^2 \quad (5)$$

where $k_n(x_1)$ and $k_n(x_2)$ are the calculation values of relative frequency shifts in the n th vibration mode to be identified and x_1 and x_2 are the positions of the two holes. In a specimen having two holes, the following identification in two steps was applied. At the first step, the first defect position x_1^0 is determined so that the coincidence factor becomes minimum, supposing a single-hole system, and then $k_n(x_1^0)$ is given by Eq. 2. Then, the second hole is searched by calculating the following coincidence factor $S(x_1^0, x_2)$ given by

$$S(x_1^0, x_2) = \sum_{n=1}^N [\{Rsfn - k_n(x_1^0)\} - k_n(x_2)]^2 \quad (6)$$

For more than three holes, Eqs. 4 and 5 can be extended to a general case by the same procedure.

Materials and methods

The effect of defects on the resonance frequency shift in the transfer matrix method was calculated for the condition that the degree of reduction of Young's modulus at the field matrix of the defect positions was 50% from the defect-free Young's modulus. Here, the reduction is equivalent to a cross-sectional loss. The number of the field matrices of the beam was chosen to be 67 to adopt the defect size of the following experiment. Then, the field matrix was replaced by the modified element successively from the end element. The following material constants were used: Young's modulus, 10 GPa; density, 0.5 g/cm³; length, 1 m; and cross section, 4.5 cm².

The number of elements greatly affects the results. To check the accuracy of calculation, the resonance frequency of a homogeneous beam calculated by the transfer matrix method was compared with its analytical solution of vibration theory for cases of different numbers of field matrices from 3 to 150. The calculation error of the resonance frequency was less than 0.001% for 67 field matrices.

Eight spruce beams (*Picea* sp.) with dimensions of 1000 × 30 × 15 mm (longitudinal, tangential, and radial directions) were used for experimental verification. The specimen density and the oven-dry moisture content were

0.44 g/cm³ and 8.8% on average, respectively. Round holes were drilled through the wide faces of each specimen. The diameter of the hole was 15 mm, that is, half the width of the specimen. Four holes were drilled finally at 1/8, 1/4, 1/3, and 1/2 positions of the specimen length, but the order of drilling was different for the four pairs of specimens. The data of each pair were averaged in the following analysis. Additional verifications were conducted for a piece of commercial structural 2 by 4 foot dimension lumber with knots. This lumber included a large knot whose knot ratio was around 0.3 at the relative distance 0.45 from an end of the lumber.

A FFT spectrum analyzer was used to obtain power spectra. Specimens were supported on pieces of foamed polyurethane. FFT utilized the standard function of the Cooley–Tukey type algorithm of the FFT spectrum analyzer. The frequency resolution increases with increase of the number of vibration modes. The maximum error in the fundamental vibration is estimated to be around 1% and those of the overtones are smaller. To diminish the restriction of free vibration by the support system, the odd-numbered vibration was measured by supporting the specimen at the center and the other vibration mode was measured by supporting it at the nodal positions of the second-numbered vibration mode.

Results and discussion

Simulation by the transfer matrix method

Figure 1 shows the resonance frequency shifts from the fundamental to the fifth modes. The calculated values were symmetrical with respect to the center position. Then, only the values over the half-span of the beam between $0 \leq x \leq 0.5$ were shown. In each vibration mode, the frequency shift is large when the defect position coincides with the node of vibration, and no shift occurs when it coincides with the loop of vibration. The magnitude of the maximum frequency shift was 1.47%.

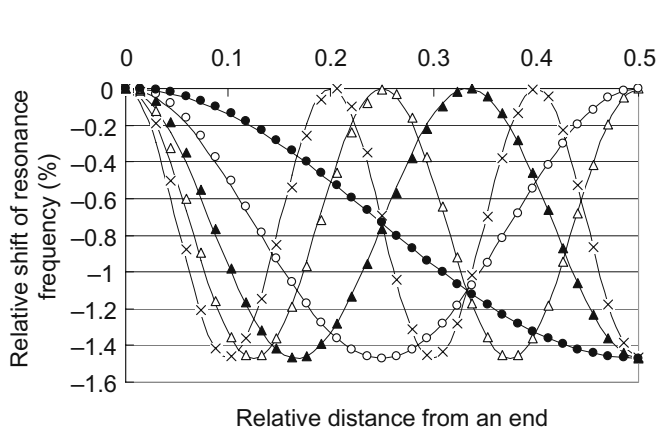


Fig. 1. Relative shift of resonance frequency by a hole calculated from the transfer matrix method. *Solid lines* show approximation by sinusoidal curves in Eq. 8. *Filled circle*, First mode; *open circle*, second mode; *filled triangle*, third mode; *open triangle*, fourth mode; *cross*, fifth mode

The frequency shift at an arbitrary defect position $k_n(x)$ was approximated by a sinusoidal curve.

$$k_n(x) = \frac{a}{2} \cos(2n\pi x) - \frac{a}{2} \quad (7)$$

where a is a maximum amplitude of the frequency shift and n is the number of vibration mode.

The approximated curves by cosine functions are also shown by solid lines in Fig. 1. The curves give a good fit to the calculation results by the transfer matrix method. The pooled data gave the following equation:

$$k_n(x) = \frac{1.47}{2} \{ \cos(2n\pi x) - 1 \}. \quad (8)$$

Effect of the positions and number of holes on the frequency shift

Figure 2 shows the effect of hole position on the frequency shift of the spectrum peak when four holes are drilled successively in the order of the 1/2, 1/3, 1/8 and 1/4 positions of the beam length. In the first drilling at the 1/2 position, peak shifts of the odd-numbered vibration modes occurred. However, those of the even-numbered modes did not occur. In the second drilling at the 1/3 position, additional frequency shifts occurred at the first, second, fourth, and fifth numbered modes. However, the shift of the third numbered vibration mode did not occur. In the third drilling at the 1/8 position, the peak shift of the fourth numbered vibration mode occurred greatly, and large shifts occurred at the second and the third numbered vibration modes; that of the fifth numbered vibration mode was slight. In the last drilling at the 1/4 position, a large shift occurred at the second numbered vibration mode, and slight shifts occurred at the odd-numbered vibration modes. However, no shift occurred at the fourth numbered vibration mode. These results show that a large frequency shift occurs when the hole position

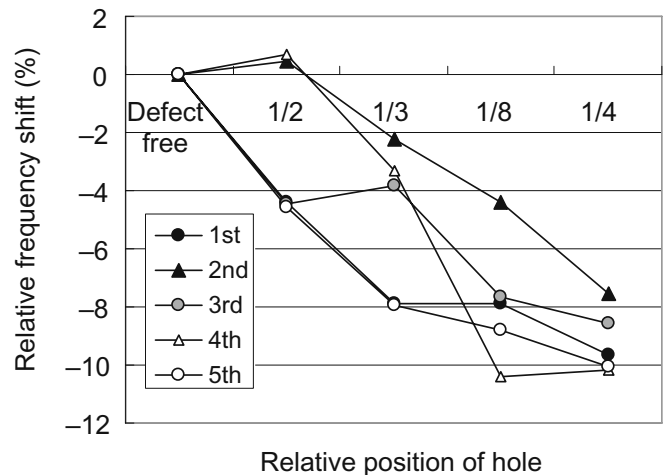


Fig. 2. Effect of hole position on relative frequency shift. Four holes are drilled successively in the order of 1/2, 1/3, 1/8, and 1/4 positions of the beam length from an end

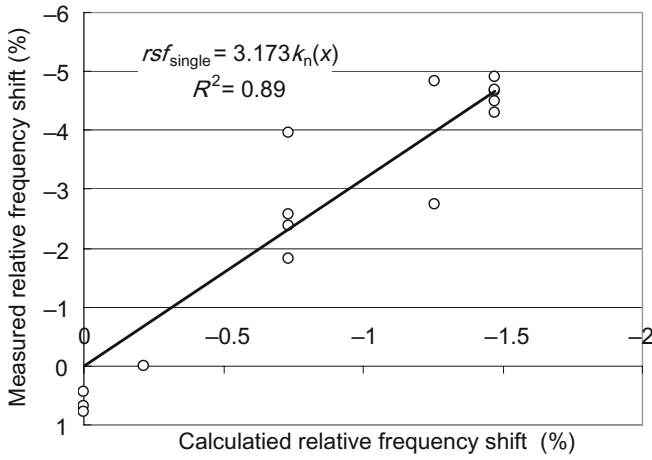


Fig. 3. Relationship between relative frequency shift by the experimental rsf_{single} and that by the calculation $k_n(x)$

coincided with the node of each vibration mode and that the shift did not occur when it coincided with the loop of each vibration mode. In the other cases, frequency shifts occur more or less according to the position of defects. A slight increase of the resonance frequency is shown at the 1/2 position of the even vibration modes. A loss of mass at a hole position can induce an increase of the resonance frequency for a combination of the hole position and the vibration mode. The same phenomenon has been reported in flexural vibration by Nakayama.¹

Prediction of relative frequency shifts

Single-hole case

Figure 3 shows the relationship between the relative frequency shift by the experimental rsf_{single} and the calculated $k_n(x)$. The following regression line was obtained for pooled data from the fundamental to fifth ordered vibration modes of single-hole specimens:

$$rsf_{\text{single}} = 3.173k_n(x) \quad (R^2 = 0.89) \quad (9)$$

The correlation coefficient of determination, R^2 , was very high, but the magnitude of the calculation value was about 30% of the experimental value rsf_{single} ; this may be the result of the effect of stress concentration around a hole, which was ignored in the transfer matrix calculation. The same effect has been reported in flexural vibration by Nakayama.¹

Multiple-hole case

The following test was done to verify the additional low on the relative frequency shift for multiple holes. The estimation of the relative frequency shift of the single hole rsf_{single} is given by substituting Eq. 8 in Eq. 9:

$$rsf_{\text{single}} = 2.332(\cos 2n\pi x - 1) \quad (10)$$

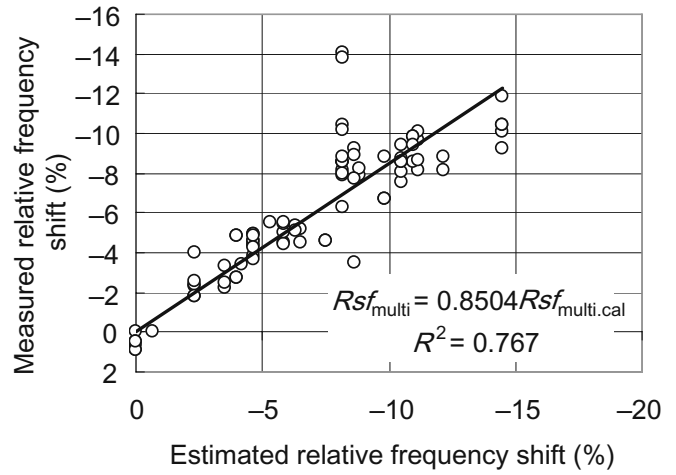


Fig. 4. Relationships between relative frequency shift by experimental Rsf_{multi} and by the additional low based on the data of a single hole $Rsf_{\text{multi.cal}}$

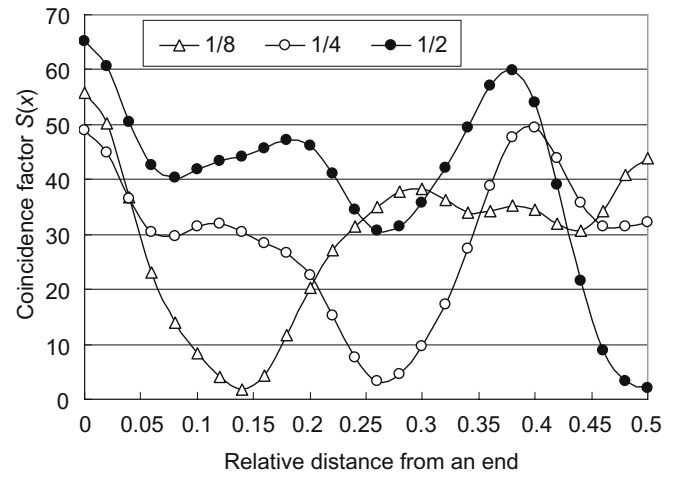


Fig. 5. Identification of a single hole drilled at 1/2, 1/4, and 1/8 positions of the beams

The relationship between the relative frequency shift by the experimental Rsf_{multi} and by the additional low based on the data of the single-hole $Rsf_{\text{multi.cal}}$ is shown in Fig. 4. The data were pooled from those of the first to fourth holes and the fundamental to fifth vibration modes.

$$Rsf_{\text{multi}} = 0.8504Rsf_{\text{multi.cal}}, \quad R^2 = 0.767 \quad (11)$$

The experimental values are 85% of the calculation values, applying the additional low, and the coefficient of determination is sufficiently large. The linearity in Eq. 11 proves the validity of the additional low in the frequency shift.

Identification of the defect position

Application to the single-hole case

Figure 5 shows the results when the single hole was drilled at 1/2, 1/4, and 1/8 positions of the beams, respectively.

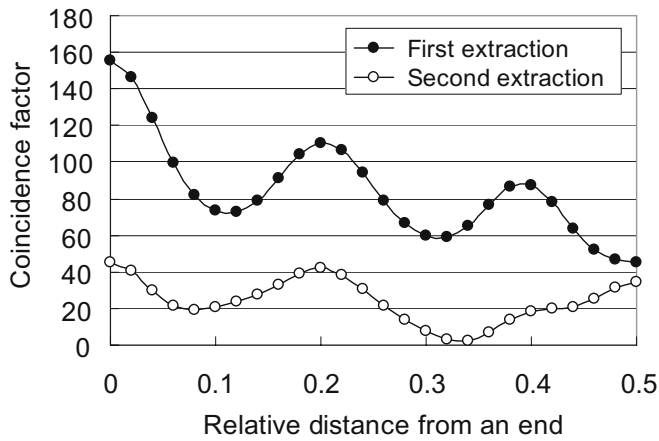


Fig. 6. Identification of two holes drilled at 1/2 and 1/3 positions of the beam

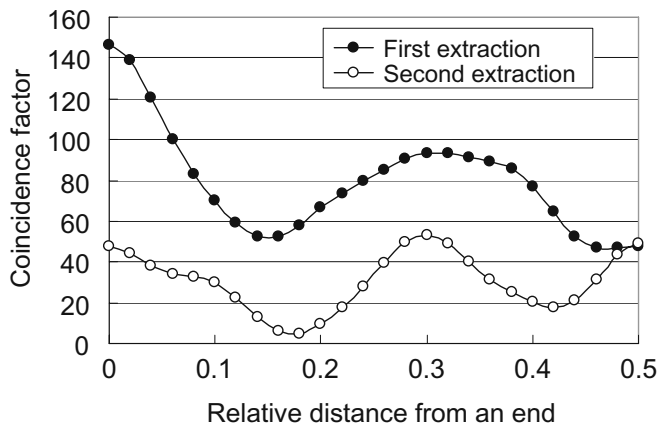


Fig. 7. Identification of two holes drilled at 1/2 and 1/8 positions of the beam

Minimum values of the coincidence factor $S(x)$ were located at each hole position. The coincidence factor was sufficiently small, and clear identification of the hole position was shown.

Application to the two-holes case

Figures 6 and 7 show the results when two holes were drilled at 1/2 and 1/3 positions and 1/2 and 1/8 positions of the beams, respectively. These holes were identified by two steps. In Fig. 6, the first hole was detected at the 1/2 position because the coincidence factor was minimum at the center of the beam. Applying Eq. 6, the second hole was detected near the 1/3 position of the beam. In Fig. 7, the first hole is detected at the center and the second one is searched at the 0.17 position of the beam. The second hole was searched as slightly inside the 1/8 position. The multiple-step identification worked efficiently. However, the resolutions of the third holes were not sufficient, because the coincidence factor became rather larger than those of the second searches. Thus, the number of holes to be identified was limited to two.

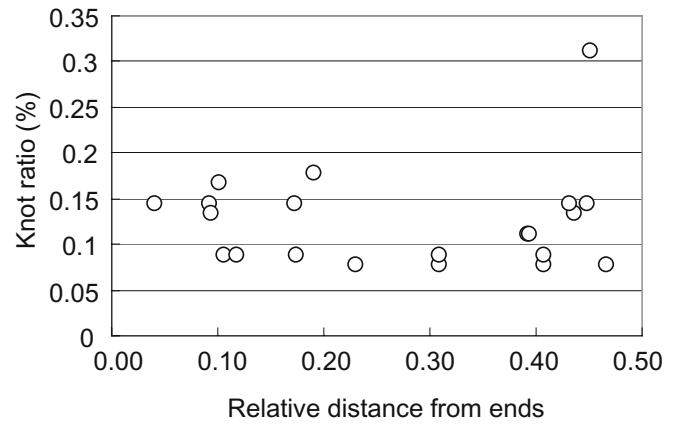


Fig. 8. Location of knots from ends in the 2 × 4 in. lumber through the length

Application to structural lumber having knots

Commercial lumber may include defects such as knots. The resonance frequencies of all vibration modes can be shifted by existence of knots. Therefore, a difficult problem in this case is “What is the fundamental resonance frequency in the defect-free condition of each piece of lumber?” Here, the following maximum frequency in the normalized resonance frequency fr_n/n among the five vibration modes was chosen as a standard frequency, fr^* .

$$fr^* = \max(fr_n/n; n = 1, 2, 3, \dots, 5) \quad (14)$$

$$rsf_n^* = \frac{fr_n/n - fr^*}{fr^*} \times 100 \quad (15)$$

This procedure was applied to a piece of 2 × 4 in. structural lumber that has a large knot near the center, whose knot ratio was 0.31 at the relative distance 0.45 from an end of the lumber. Figure 8 shows the location of knots through the length in the same piece of lumber. The relative frequency shifts of the standard frequency at the first to fifth vibration modes were −3.147%, 0%, −3.263%, −1.224%, and −2.098%, respectively. The frequency shifts of the first and third modes were large, that of the fifth mode was moderately large, and those of the even modes were small. This result means that a predominant knot will locate near the center of the lumber. In Fig. 9, the knot was searched at the relative distance 0.45. In the second search, the coincidence factor became rather larger than in the first search, which means that the second defect is neither predominant nor negligible compared with the first defect.

Conclusions

The inverse solution procedure that enables the identification of the defect position from the power spectrum of the longitudinal vibration was exploited. It is composed of the estimation of the frequency shift, which was calculated by the transfer matrix method, and the coincidence test, which searched the optimal solution between the experiment and

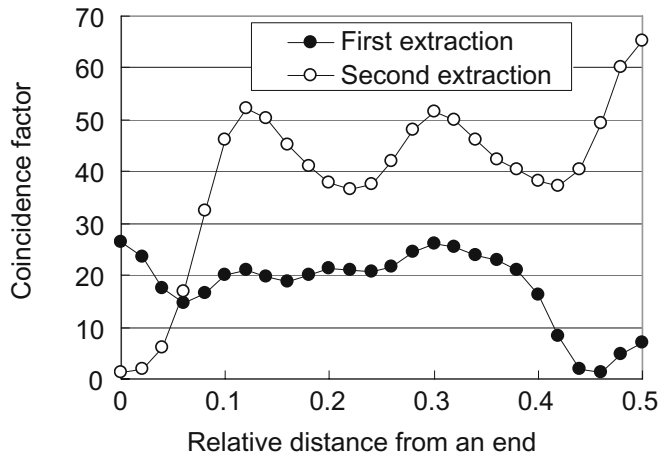


Fig. 9. Identification of knot location from an end in the 2×4 in. structural lumber

the calculation. The defect position was well identified, but the procedure was limited to the identification of two dominant defects.

References

- Nakayama Y (1974) Vibrational property of wooden beam containing the decrease section (in Japanese). *Mokuzai Gakkaishi* 20:1–8
- Sobue N, Nakano A (2001) Flattering of the resonance frequency by defects in wood in the longitudinal tapping method. Abstracts of the 51st Annual Meeting of the JWRS, p 91
- Brancheriau L, Bailleres H, Sale C (2006) Acoustic resonance of xylophone bars: experimental and analytic approach of frequency shift phenomenon during the tuning operation of xylophone bars. *Wood Sci Technol* 40:94–106
- Nagai H, Murata K, Nakamura M (2007) Defect determination of lumber including knots using bending deflection curve. *J Soc Mater Sci, Japan* 56:326–331
- Yang X, Ishimaru Y, Iida I, Urakami H (2002) Application of modal analysis by transfer function to non-destructive testing of wood I: determination of localized defects in wood by the shape of the flexural vibration wave. *J Wood Sci* 48:283–288
- Yang X, Amano T, Ishimaru Y, Iida I (2003) Application of modal analysis by transfer function to non-destructive testing of wood II: modulus of elasticity evaluation of sections of different quality in a wooden beam by the curvature of the flexural vibration wave. *J Wood Sci* 49:140–144
- Choi F C, Li J, Samali S, Crews K (2007) Application of modal-based damage-detection method to locate and evaluate damage in timber beams. *J Wood Sci* 53:394–400
- Hatter J D (1977) Matrix computer methods of vibration analysis. Translated by Washizu H. Brain Tosho Shuppan, Tokyo, pp 111–115, 160–164
- Sobue N (1990) Correction factors of the resonance frequency for tapering and shear deformation of a log in flexural vibration (in Japanese). *Mokuzai Gakkaishi* 36:760–764
- Sobue N, Ikeda K, Arima T (1988) Measurement of flexural rigidity of plywood-webbed box-beams by vibration method (in Japanese). *Mokuzai Gakkaishi* 34:543–546
- Nakao T, Kondo Y, Ohta M, Okano T (1985) Analysis of flexural vibration of wooden beams with variable thickness by the transfer-matrix method considering the effect of shear deformation (in Japanese). *Mokuzai Gakkaishi* 31:440–445